

Measurement of the decay $K_L \rightarrow \pi^0 e^+ e^- \gamma$

E. Abouzaid,⁴ M. Arenton,¹¹ A. R. Barker,^{5,*} L. Bellantoni,⁷ E. Blucher,⁴ G. J. Bock,⁷ E. Cheu,^{1,†} R. Coleman,⁷ B. Cox,¹¹ A. R. Erwin,¹² C. O. Escobar,³ A. Glazov,⁴ A. Golossanov,¹¹ R. A. Gomes,³ P. Gouffon,¹⁰ Y. B. Hsiung,⁷ D. A. Jensen,⁷ R. Kessler,⁴ Y. J. Kim,¹ K. Kotera,⁸ A. Ledovskoy,¹¹ P. L. McBride,⁷ E. Monnier,^{4,‡} K. S. Nelson,¹¹ H. Nguyen,⁷ R. Niclasen,⁵ D. G. Phillips II,¹¹ H. Ping,¹² E. J. Ramberg,⁷ R. E. Ray,⁷ M. Ronquest,¹¹ E. Santos,¹⁰ W. Slater,² D. Smith,¹¹ N. Solomey,⁴ E. C. Swallow,^{4,6} P. A. Toale,⁵ R. Tschirhart,⁷ C. Velissaris,¹² Y. W. Wah,⁴ J. Wang,¹ H. B. White,⁷ J. Whitmore,⁷ M. J. Wilking,⁵ R. Winston,⁴ E. T. Worcester,⁴ M. Worcester,⁴ T. Yamanaka,⁸ E. D. Zimmerman,⁵ and R. F. Zukanovich¹⁰

(KTeV Collaboration)

¹University of Arizona, Tucson, Arizona 85721, USA²University of California at Los Angeles, Los Angeles, California 90095, USA³Universidade Estadual de Campinas, Campinas, Brazil 13083-970⁴The Enrico Fermi Institute, The University of Chicago, Chicago, Illinois 60637, USA⁵University of Colorado, Boulder, Colorado 80309, USA⁶Elmhurst College, Elmhurst, Illinois 60126, USA⁷Fermi National Accelerator Laboratory, Batavia, Illinois 60510, USA⁸Osaka University, Toyonaka, Osaka 560-0043 Japan⁹Rice University, Houston, Texas 77005, USA¹⁰Universidade de São Paulo, São Paulo, Brazil 05315-970¹¹The Department of Physics and Institute of Nuclear and Particle Physics, University of Virginia, Charlottesville, Virginia 22901, USA¹²University of Wisconsin, Madison, Wisconsin 53706, USA

(Received 27 June 2007; published 12 September 2007)

We report on a new measurement of the branching ratio $B(K_L \rightarrow \pi^0 e^+ e^- \gamma)$ using the KTeV detector. This analysis uses the full KTeV data set collected from 1997 to 2000. We reconstruct 139 events over a background of 14, which results in $B(K_L \rightarrow \pi^0 e^+ e^- \gamma) = (1.62 \pm 0.14_{\text{stat}} \pm 0.09_{\text{syst}}) \times 10^{-8}$. This result supersedes the earlier KTeV measurement of this branching ratio.

DOI: [10.1103/PhysRevD.76.052001](https://doi.org/10.1103/PhysRevD.76.052001)

PACS numbers: 13.20.Eb, 11.30.Er, 12.39.Fe, 13.40.Gp

I. INTRODUCTION

The decay $K_L \rightarrow \pi^0 e^+ e^- \gamma$ can be used to study the low-energy dynamics of neutral K mesons. In particular, this decay is an important check of chiral perturbation theory, which has been used to describe kaon decays in which long distance effects dominate. Up to $O(p^4)$ in chiral perturbation theory, there are no free parameters and one predicts the branching ratio to be approximately 1.0×10^{-8} [1]. In the related decay $K_L \rightarrow \pi^0 \gamma \gamma$, the $O(p^4)$ calculation was found to underestimate the measured branching ratio by a factor of 3 [2–6]. To match the $K_L \rightarrow \pi^0 \gamma \gamma$ data it was found necessary to extend the calculation to include $O(p^6)$ terms while introducing a free parameter, a_V . This parameter characterizes the contributions from vector meson exchange terms [7]. The addition of these effects to the $K_L \rightarrow \pi^0 e^+ e^- \gamma$ calculation

results in an increase in the branching ratio to 2.4×10^{-8} , approximately twice the $O(p^4)$ calculation. Our new branching ratio measurement can distinguish between the $O(p^4)$ and $O(p^6)$ predictions.

Two previous experimental results have been reported on this decay mode [8–10]. The most recent measurement comes from the KTeV 1997 data set and is based on 48 events with a background of 3.6 ± 1.1 events. That measurement yielded $B(K_L \rightarrow \pi^0 e^+ e^- \gamma) = (2.34 \pm 0.35 \pm 0.13) \times 10^{-8}$, where the rate was normalized to a now-obsolete value of $B(K_L \rightarrow \pi^0 \pi^0)$. Using the latest measurement of $B(K_L \rightarrow \pi^0 \pi^0)$ [11,12], the 1997 measurement can be rescaled to $(2.17 \pm 0.32 \pm 0.12) \times 10^{-8}$. We report here on a new measurement of this mode from the KTeV experiment. For this analysis, we use improved techniques to reanalyze the 1997 data set and combine it with a new measurement from the 1999 data set.

The $K_L \rightarrow \pi^0 e^+ e^- \gamma$ decay can also be used to help understand the CP violating decay, $K_L \rightarrow \pi^0 e^+ e^-$. The $K_L \rightarrow \pi^0 e^+ e^-$ decay contains both CP violating and CP conserving amplitudes. Since the $K_L \rightarrow \pi^0 e^+ e^- \gamma$ decay proceeds through a two photon intermediate state, it can be

*Deceased.

†To whom correspondence should be addressed.
elliott@physics.arizona.edu

‡Permanent address: C.P.P. Marseille/C.N.R.S., France.

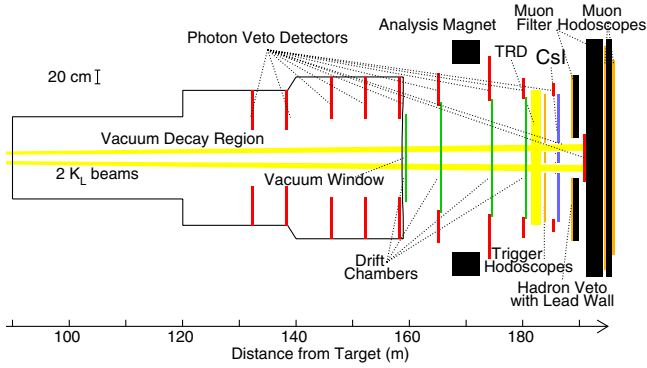


FIG. 1 (color online). Schematic of the KTeV detector.

used to determine the CP conserving components in $K_L \rightarrow \pi^0 e^+ e^-$, and thus allow one to determine the CP violating contribution in $K_L \rightarrow \pi^0 e^+ e^-$. Also, because the rate for $K_L \rightarrow \pi^0 e^+ e^- \gamma$ is orders of magnitude higher than the rate for $K_L \rightarrow \pi^0 e^+ e^-$, a better understanding of the $K_L \rightarrow \pi^0 e^+ e^- \gamma$ decay will help to reduce the backgrounds to the $K_L \rightarrow \pi^0 e^+ e^-$ decay.

II. THE KTeV DETECTOR

We collect $K_L \rightarrow \pi^0 e^+ e^- \gamma$ events using the KTeV detector located at Fermilab. The KTeV detector is shown in Fig. 1. The data analyzed were taken during the 1997 and 1999 rare decay running periods and comprised 2.9×10^{11} and 3.8×10^{11} kaon decays, respectively. The KTeV experiment employed two different configurations during its operation. The E799 configuration was used for this measurement and was optimized for reconstructing rare kaon decays.

In the KTeV experiment [13] neutral kaons are produced in interactions of 800 GeV/ c protons with a beryllium oxide target. The resulting particles pass through a series of collimators to produce two nearly parallel beams. The beams also pass through lead and beryllium absorbers to reduce the fraction of photons and neutrons in each beam. Charged particles are removed from the beams by sweeping magnets located downstream of the collimators. The vacuum decay volume begins approximately 94 m downstream of the target, far enough so that the majority of the K_S mesons have decayed, and extends to approximately 159 m from the target. The decay volume is surrounded by photon veto detectors that reject photons at angles greater than 100 mrad.

The most critical detector elements for this analysis are a charged particle spectrometer and a pure CsI electromagnetic calorimeter [14]. The KTeV spectrometer is used for reconstructing charged tracks. This spectrometer consists of four planes of drift chambers, two located upstream and two downstream of an analyzing magnet with a transverse momentum kick of 0.205 GeV/ c . Each drift chamber contains four planes of wires, two to measure the horizontal

position and two to measure the vertical position with a precision of approximately 100 μm . During data taking in 1999 the momentum kick was reduced to 0.150 GeV/ c to increase the acceptance for multitrack events.

The CsI calorimeter is composed of 3100 blocks in a 1.9 m by 1.9 m array. The depth of the CsI calorimeter corresponds to 27 radiation lengths. Two 15 cm by 15 cm holes are located near the center of the array for the passage of the two neutral beams. For electrons with energies between 2 and 60 GeV, the calorimeter energy resolution is below 1% and the nonlinearity is less than 0.5%. The position resolution of the calorimeter is approximately 1 mm. Downstream of the CsI calorimeter, there is a 10 cm lead wall, followed by a hodoscope used to reject hadrons hitting the calorimeter.

The $K_L \rightarrow \pi^0 e^+ e^- \gamma$ decays were required to satisfy certain trigger requirements in order to be recorded. In particular, activity in a set of hodoscopes upstream of the CsI calorimeter had to be consistent with two tracks. Also, we required the event have at least one hit in one of the two upstream drift chambers. The event must deposit more than approximately 25 GeV of total energy in the CsI calorimeter and no more than 0.5 GeV in the photon vetoes. The event is vetoed if it deposits more than 2.5 Mips in the hodoscope downstream of the calorimeter or more than 14 GeV in the vetos around the beam holes in the CsI calorimeter. The trigger includes a hardware cluster processor that counts the number of in-time calorimeter clusters of contiguous blocks of CsI with energies above 1 GeV [15]. The total number of electromagnetic clusters in the CsI calorimeter is required to be greater than or equal to four at the trigger level.

After the events are read out, they must satisfy a software filter. This filter requires that each event have two charged tracks with a minimum of four clusters in the calorimeter. Each of the tracks must point to a cluster in the calorimeter and be consistent with an electron hypothesis. The trigger requirements also select $K_L \rightarrow \pi^0 \pi_D^0$ events where one neutral pion undergoes Dalitz decay, $\pi^0 \rightarrow e^+ e^- \gamma$ (π_D^0). These events are used for normalizing the $K_L \rightarrow \pi^0 e^+ e^- \gamma$ events, since their topology is very similar to that of our signal events. Because of the similarity in topologies between the signal and normalization modes, many systematic effects cancel.

III. EVENT RECONSTRUCTION

The offline analysis begins by requiring that each event have exactly two oppositely signed tracks and five in-time clusters with energies greater than 2.0 GeV, where an in-time cluster is one in which the cluster reconstructs to within 19 ns of the event time. The two tracks are required to point to two of the clusters and be consistent with a common decay vertex. From the three neutral clusters, we combine two to form the π^0 candidate. There are three possible combinations, and we choose the combination

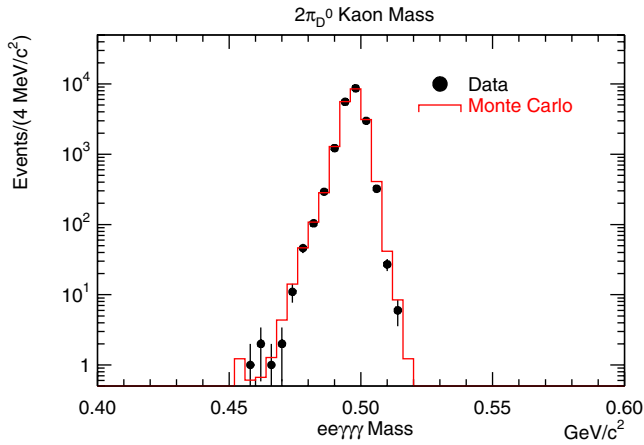


FIG. 2 (color online). The $K_L \rightarrow \pi^0 \pi_D^0$ invariant mass distribution for data (dots) and $K_L \rightarrow \pi^0 \pi_D^0$ Monte Carlo (solid histogram).

that reconstructs closest to the π^0 mass. Only events with a $\gamma\gamma$ invariant mass within $5 \text{ MeV}/c^2$ of the nominal π^0 mass are accepted. The neutral decay distance vertex is used to determine the mass of the $e^+e^-\gamma$ and $e^+e^-\gamma\gamma$ combinations because it improves their mass resolution; the e^+e^- tracks tend to be close together leading to poorer vertex resolution. The total kaon energy, determined from the sum of cluster energies in the calorimeter, must lie between 30 and 210 GeV.

To ensure that the two tracks are electrons, the reconstructed energy in the calorimeter divided by the momentum determined by the spectrometer (E/p) of each track must be between 0.95 and 1.05. Backgrounds from K_S decays and misreconstructed kaons can be reduced by requiring the decay vertex to reconstruct between 98 and 157 m downstream of the target, and the transverse momentum squared (p_T^2) for the event to be less than $0.003(\text{GeV}/c)^2$. The invariant mass for $K_L \rightarrow \pi^0 \pi_D^0$ events is shown in Fig. 2. The data and our Monte Carlo simulation agree quite well.

IV. BACKGROUNDS TO $K_L \rightarrow \pi^0 e^+ e^- \gamma$

After applying the above selection criteria, the remaining backgrounds consist mainly of $K_L \rightarrow \pi^0 \pi_D^0$ and $K_L \rightarrow \pi^0 \pi^0 \pi_D^0$ decays. The $K_L \rightarrow \pi^0 \pi_D^0$ decays are more readily removed because the invariant masses of the $e^+e^-\gamma$ and $\gamma\gamma$ combinations reconstruct around the mass of the π^0 . The majority of the $K_L \rightarrow \pi^0 \pi_D^0$ events are removed by requiring the reconstructed $e^+e^-\gamma$ mass of the best combination to be less than $0.110 \text{ GeV}/c^2$ or greater than $0.155 \text{ GeV}/c^2$. However, when the wrong $\gamma\gamma$ combination is chosen, a restriction on the invariant masses is ineffective at reducing the background. $K_L \rightarrow \pi^0 \pi_D^0$ events can also contribute to the background if one of the final state particles is lost and is replaced by activity in the detector that can mimic a final state particle. The $K_L \rightarrow \pi^0 \pi^0 \pi_D^0$

events are more difficult to remove because we cannot use the same mass constraints as in the $K_L \rightarrow \pi^0 \pi_D^0$ case. However, kinematic and cluster shape variables have been developed to help to reduce the background to a manageable level.

To remove misreconstructed $K_L \rightarrow \pi^0 \pi_D^0$ decays, we consider the two other possible $\gamma\gamma$ combinations. We take advantage of the correlations between the $m_{\gamma\gamma}$ and $m_{e^+e^-\gamma}$ distributions for these two combinations, forming a neural net from four variables. These four input variables are the reconstructed invariant $\gamma\gamma$ and $e^+e^-\gamma$ masses for each of the two remaining combinations. The neural net employed 16 hidden nodes and was tuned on a sample of $2\pi_D^0$ and $\pi^0 e^+e^-\gamma$ Monte Carlo. The output from the neural net ranges between zero and one. We rejected events where the neural net value was less than 0.5.

Backgrounds from $K_L \rightarrow \pi^0 \pi^0 \pi_D^0$ come from two broad classes of events: events with missing photons and those with one or more photons that overlap or fuse together in the CsI calorimeter. For events with missing photons, we use the photon vetoes to significantly reduce the amount of background. We require the maximum energy in any photon veto to be less than 0.1 GeV. To reduce backgrounds from events with overlapping photons, we examined the calorimeter energies in a 3×3 array of crystals centered around the highest energy crystal of the

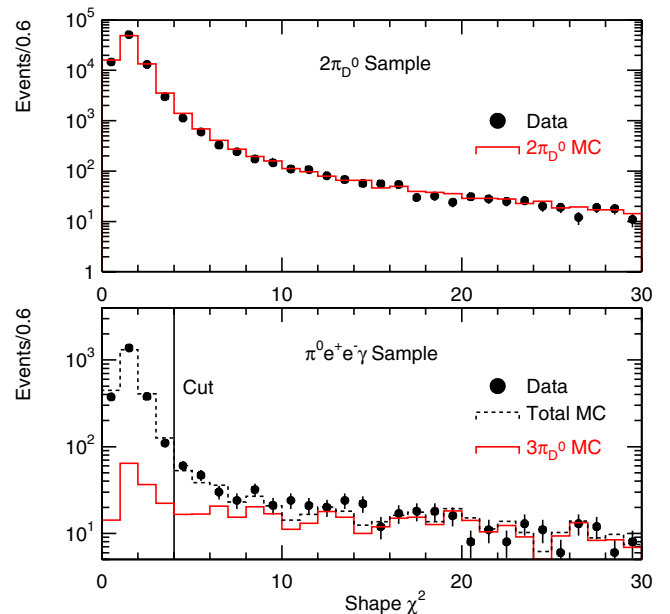


FIG. 3 (color online). The photon shape variable shape χ^2 . The top plot shows the shape χ^2 variable for $K_L \rightarrow \pi^0 \pi_D^0$ with the dots representing the data and the solid histogram the Monte Carlo. In the bottom histogram the dots are the data after removing the $K_L \rightarrow \pi^0 \pi_D^0$ events, while the solid histogram shows the $K_L \rightarrow \pi^0 \pi^0 \pi_D^0$ Monte Carlo. The dashed histogram represents the sum of the signal and background Monte Carlo samples.

cluster. For reference, a 3×3 array corresponds to approximately one Molière radius. We compared these energies to energies from an ideal cluster shape and calculated a photon shape χ^2 variable. This variable is shown in Fig. 3. As can be seen, for the normalization mode, there is good agreement in this variable between the data and the Monte Carlo simulation. For the signal events, the background from $K_L \rightarrow \pi^0 \pi^0 \pi_D^0$ events is significantly reduced by requiring a small value of shape χ^2 . We require shape $\chi^2 < 4$.

Kaon decays with missing photons will also exhibit a significant amount of missing energy when boosted to the center-of-mass. We take advantage of this effect by calculating the longitudinal missing momentum in the center-of-mass (pp0kine). In the pp0kine versus $m_{\gamma\gamma\gamma}$ plane, the signal events are well-separated from the $K_L \rightarrow \pi^0 \pi^0 \pi_D^0$ background. We define a two dimensional cut by employing the following fourth-order polynomial:

$$\text{pp0kine}_{\text{max}} = A + B * (m_{\gamma\gamma\gamma} - x_0) + C * (m_{\gamma\gamma\gamma} - x_0)^2 + D * (m_{\gamma\gamma\gamma} - x_0)^3 + E * (m_{\gamma\gamma\gamma} - x_0)^4,$$

where $A = 3.9$, $B = -112.8$, $C = 1256.6$, $D = -5861.8$, $E = 10\,506.0$, and $x_0 = 8.326 \times 10^{-2}$. The values of these parameters were chosen to maximize the signal-to-background ratio. Events with values of pp0kine greater than this value were rejected. This cut is shown in Fig. 4.

Both $K_L \rightarrow \pi^0 \pi_D^0$ and $K_L \rightarrow \pi^0 \pi^0 \pi_D^0$ events can contribute to the final data sample if one of the electrons undergoes bremsstrahlung radiation. To reduce this background, we calculate the minimum distance between the

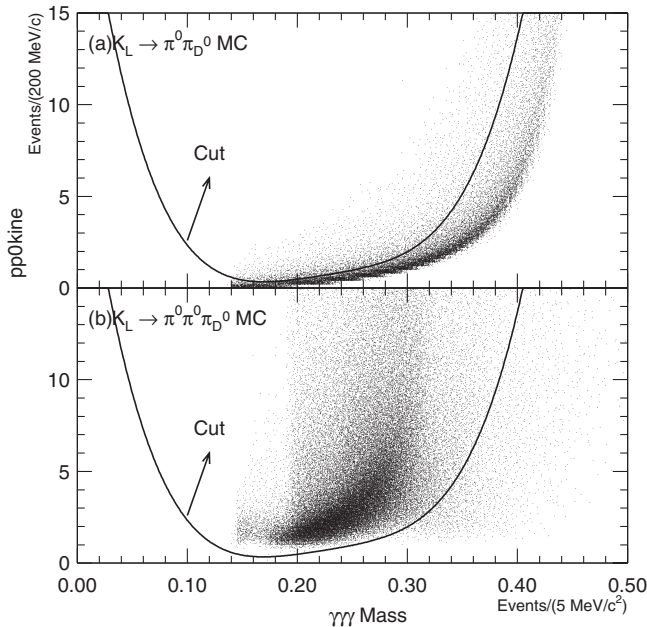


FIG. 4. The pp0kine variable plotted versus the $\gamma\gamma\gamma$ invariant mass for (a) $K_L \rightarrow \pi^0 \pi_D^0$ and (b) $K_L \rightarrow \pi^0 \pi^0 \pi_D^0$ Monte Carlo events. The dark line represents the cut indicated in the text.

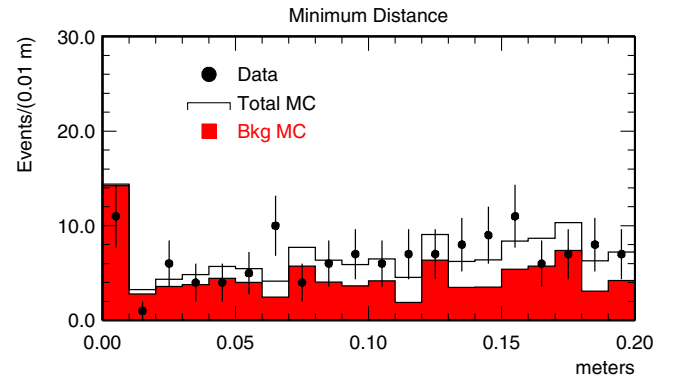


FIG. 5 (color online). The minimum distance between the projection of the upstream electron track segment to the CsI calorimeter and any photon candidate. The dots represent the data and the solid histogram the sum of the background and signal Monte Carlo. The enhancement at low values of the minimum distance is the result of bremsstrahlung production.

projection of the upstream segment of each electron to the CsI calorimeter and any photon cluster. Bremsstrahlung photons tend to have a small minimum distance. As shown in Fig. 5, backgrounds from $K_L \rightarrow \pi^0 \pi_D^0$ and $K_L \rightarrow \pi^0 \pi^0 \pi_D^0$ occur at small photon-to-track distances. To reduce this background, we require the minimum distance to be greater than 1.25 cm.

Backgrounds due to external conversions of photons are negligible since we require the decay vertex to lie within the vacuum decay region, upstream of the vacuum window. The requirement that the neutral and charged vertex be consistent with each other further reduces the probability of external conversions contributing to the background since external conversions can only result from interactions with material downstream of the vacuum window.

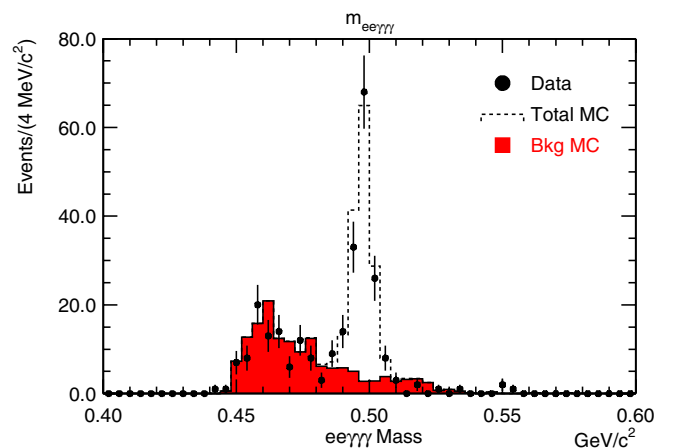


FIG. 6 (color online). The $e^+ e^- \gamma\gamma\gamma$ invariant mass for events passing all selection criteria. The dots represent the data, while the dashed histogram represents the sum of the signal and background Monte Carlo. The background Monte Carlo is indicated by the shaded histogram.

V. RESULTS

After making these final selection criteria, we find the $e^+e^-\gamma\gamma\gamma$ mass distributions shown in Fig. 6. A clear peak at the kaon mass is seen, while the background is well-described by the sum of the $2\pi_D^0$ and $3\pi_D^0$ background Monte Carlo samples. We find a total of 139 candidate events with an estimated background of 14.4 ± 2.5 events.

The $K_L \rightarrow \pi^0 e^+ e^- \gamma$ branching fraction is determined from the following expression:

$$B = (N_{\pi^0 e^+ e^- \gamma} / N_{2\pi^0}) \times (\epsilon_{2\pi^0} / \epsilon_{\pi^0 e^+ e^- \gamma}) \\ \times B(K_L \rightarrow \pi^0 \pi^0) \times B(\pi^0 \rightarrow e^+ e^- \gamma) \times 2.$$

Here, $N_{\pi^0 e^+ e^- \gamma}$ represents the number of signal candidates, while $N_{2\pi^0}$ represents the number of normalization events. The number of $K_L \rightarrow \pi^0 \pi_D^0$ candidates is determined by inverting the cut against $K_L \rightarrow \pi^0 \pi_D^0$ events and counting the number of events in the kaon mass region from 0.490 to 0.510. In the above expression $\epsilon_{2\pi^0}$ and $\epsilon_{\pi^0 e^+ e^- \gamma}$ correspond to the reconstructed $K_L \rightarrow 2\pi^0$ and $K_L \rightarrow \pi^0 e^+ e^- \gamma$ acceptances, respectively. The factor of 2 occurs because there are two π^0 in each $K_L \rightarrow \pi^0 \pi_D^0$ event. In the previous analysis, the value of $B(K_L \rightarrow \pi^0 \pi^0)$ used was $(9.36 \pm 0.2) \times 10^{-4}$. We are now using the most recent determination of $B(K_L \rightarrow \pi^0 \pi^0) = (8.69 \pm 0.08) \times 10^{-4}$. The value of $B(\pi^0 \rightarrow e^+ e^- \gamma)$ used in both analyses is $(1.198 \pm 0.032) \times 10^{-2}$.

The acceptance for $K_L \rightarrow 2\pi_D^0$ events is 0.51% in the 1997 data set and 0.61% in the 1999 data set. The difference between the acceptances in the two data sets arises from the different magnetic fields used during the 1997 and 1999 runs. We find 31 286 $K_L \rightarrow \pi^0 \pi_D^0$ events in the 1997 data and 49 159 events in the 1999 data. This corresponds to a kaon flux of 2.92×10^{11} and 3.84×10^{11} decays in the 1997 and 1999 data sets, respectively. The $\pi^0 e^+ e^- \gamma$ acceptances are 1.02% and 1.18% for the 1997 and 1999 data sets, respectively. These values are shown in Table I. Using the numbers above, we obtain:

$$B(K_L \rightarrow \pi^0 e^+ e^- \gamma) = (1.49 \pm 0.22) \times 10^{-8} \quad (1997),$$

$$B(K_L \rightarrow \pi^0 e^+ e^- \gamma) = (1.77 \pm 0.18) \times 10^{-8} \quad (1999).$$

The difference between the result in Ref. [10] and our new 1997 measurement of the $K_L \rightarrow \pi^0 e^+ e^- \gamma$ branching ratio can be mainly attributed to the different values of a_V used

in determining the acceptance. The previous measurement used $a_V = -0.96$ while our new analysis uses $a_V = -0.46$ [6]. After accounting for this acceptance effect, we find that the two analyses are consistent with each other. Our new measurement supersedes the previous KTeV measurement.

VI. SYSTEMATIC UNCERTAINTIES

The largest systematic uncertainty results from the limited statistics in our background Monte Carlo sample. In total we generated approximately twice the statistics of the $K_L \rightarrow \pi^0 \pi^0 \pi_D^0$ data sample, and approximately 3 times the statistics of the normalization and signal modes. This required generating about 6×10^9 Monte Carlo events. The next largest systematic uncertainty arises from the K_L and $\pi^0 \rightarrow e^+ e^- \gamma$ branching ratios. The remaining effects can be broken down into two main classes: those that affect the background level and those that affect the signal or normalization acceptance. The signal acceptance has a dependence upon the value of a_V . This dependence can be characterized by $B = 1.484 + 0.215 * a_V + 0.1170 * a_V^2 + 0.417 * a_V^3$. We varied the value of a_V between -0.41 and -0.51 [6], and found the acceptance changed by approximately 2.0%. The uncertainty in the background contributes approximately 0.5% to the total systematic uncertainty, and the remaining acceptance effects including the effects of apertures and cuts contribute about 0.6% to the total systematic error. All of the systematic errors are listed in Table II.

To obtain the final result, we took the weighted average of the 1997 and 1999 numbers, where we weighted by the statistical error. The systematic studies were done on the combined 1997 and 1999 analyses to take into account any correlations. Including the uncertainties due to the systematic effects, we find the following result: $B(K_L \rightarrow \pi^0 e^+ e^- \gamma) = (1.62 \pm 0.14_{\text{stat}} \pm 0.09_{\text{syst}}) \times 10^{-8}$.

The relatively small value for the $K_L \rightarrow \pi^0 e^+ e^- \gamma$ branching ratio means that this decay will not serve as a significant source of background to $K_L \rightarrow \pi^0 e^+ e^-$. The $\pi^0 e^+ e^-$ mass distribution from $K_L \rightarrow \pi^0 e^+ e^- \gamma$ decays peaks around $0.250 \text{ GeV}/c^2$, far enough away from the kaon mass that only a small fraction of the decays pose any risk of reconstructing in the $K_L \rightarrow \pi^0 e^+ e^-$ signal region.

To determine the value of a_V from our data, we performed a maximum likelihood fit to the three Dalitz pa-

TABLE I. Values used in branching ratio calculation.

Value	1997	1999
Events in Data	47	92
Background Events	2.7	11.7
Normalization Events	31 286	49 159
Signal Acceptance	1.02%	1.18%
Normalization Acceptance	0.51%	0.61%

TABLE II. Systematic uncertainties in percent.

Systematic	Error (%)
MC Statistics	4.2
$K_L \rightarrow \pi^0 \pi^0$ and π_D^0 BR	2.8
a_V dependence	2.0
Signal acceptance	0.6
$3\pi_D^0$ and $2\pi_D^0$ background	0.5
Total	5.2

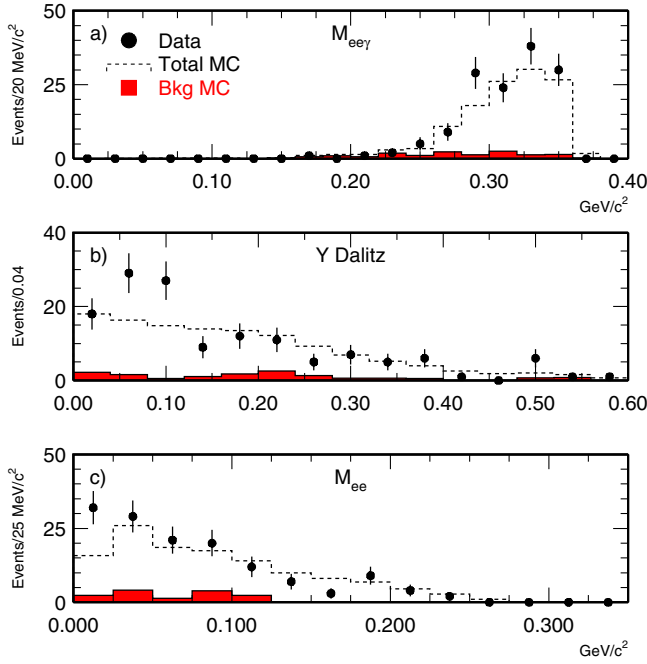


FIG. 7 (color online). The Dalitz variables used in the fit for a_V : (a) $m_{e^+e^- \gamma}$, (b) Y , and (c) $m_{e^+e^-}$. The dots are the data. The dashed histogram is the sum of the background and signal Monte Carlo, and the filled histogram is the background Monte Carlo.

rameters $Z = \frac{m_{e\gamma}^2}{m_K^2}$, $Q = \frac{m_{ee}^2}{m_K^2}$, and $Y = \frac{E_\gamma - E_{ee}}{m_K}$. The variables E_γ and E_{ee} are the energies of the photon and the e^+e^- pair in the kaon center-of-mass frame, respectively. The value of a_V that we obtained is $-0.76 \pm 0.16 \pm 0.07$. The major systematics are the background level and the sensitivity to the selection criteria. Our value for a_V is consistent with the recent published values but our errors are significantly larger. The distributions of the Dalitz variables are shown in Fig. 7. We find good agreement between the data and the Monte Carlo generated with the central a_V value. The shapes of the $m_{e^+e^- \gamma}$ and Y variables are similar to those seen in $K_L \rightarrow \pi^0 \gamma \gamma$ decay. In principle the e^+e^- mass distribution should rise sharply near threshold. However, due to the detector acceptance this peaking is suppressed.

In Ref. [1] the $O(p^6)$ calculation predicts the $K_L \rightarrow \pi^0 e^+ e^- \gamma$ branching ratio to be 2.4×10^{-8} . This prediction depends upon the value of a_V . For a value of $a_V = -0.46$ the branching ratio prediction is 1.51×10^{-8} , which is consistent with our measurement. The $O(p^4)$ calculation, meanwhile, predicts a branching ratio of 1×10^{-8} . Therefore, our latest measurement disfavors the $O(p^4)$ prediction while favoring the $O(p^6)$ calculation.

VII. CONCLUSIONS

We have determined the branching ratio $B(K_L \rightarrow \pi^0 e^+ e^- \gamma)$ using the combined 1997 and 1999 data sets from the KTeV experiment. The statistics represents a factor of 2.5 over our published 1997 result. Compared to our previous result, this analysis utilizes a number of new analysis techniques and employs an improved understanding of the backgrounds. We determine the branching ratio to be $B(K_L \rightarrow \pi^0 e^+ e^- \gamma) = (1.62 \pm 0.14_{\text{stat}} \pm 0.09_{\text{syst}}) \times 10^{-8}$. The most recent measurement of a_V [6] suggests that the decay $K_L \rightarrow \pi^0 e^+ e^-$ is dominated by a CP violating amplitude. While the statistics are low, the value of a_V from our determination is consistent with these conclusions. Our branching ratio measurement confirms the value of a_V measured by NA48 and indicates that $O(p^6)$ terms are important for modeling this decay mode. The measured branching ratio is within 0.7σ of the $O(p^6)$ prediction and about 3.7σ from the $O(p^4)$ prediction. A factor of 20 increase in the statistics of $K_L \rightarrow \pi^0 e^+ e^- \gamma$ would make the measurement of a_V competitive with the current best measurements. Because of the kinematics and small branching ratio for $K_L \rightarrow \pi^0 e^+ e^- \gamma$, this decay will not constitute a large background in future searches for $K_L \rightarrow \pi^0 e^+ e^-$.

ACKNOWLEDGMENTS

We gratefully acknowledge the support and effort of the Fermilab staff and the technical staffs of the participating institutions for their vital contributions. This work was supported in part by the U.S. Department of Energy, The National Science Foundation, The Ministry of Education and Science of Japan, Fundação de Amparo a Pesquisa do Estado de São Paulo-FAPESP, Conselho Nacional de Desenvolvimento Científico e Tecnológico-CNPq, and CAPES-Ministerio Educao.

- [1] J.F. Donoghue and F. Gabbiani, Phys. Rev. D **56**, 1605 (1997).
- [2] G.D. Barr *et al.*, Phys. Lett. B **242**, 523 (1990).
- [3] V. Papadimitriou *et al.*, Phys. Rev. D **44**, R573 (1991).
- [4] G.D. Barr *et al.*, Phys. Lett. B **284**, 440 (1992).
- [5] A. Alavi-Harati *et al.*, Phys. Rev. Lett. **83**, 917 (1999).

- [6] A. Lai *et al.*, Phys. Lett. B **536**, 229 (2002).
- [7] G. D'Ambrosio and J. Portoles, Nucl. Phys. **B492**, 417 (1997).
- [8] G. Graham, Ph.D. thesis, University of Chicago 1999.
- [9] K. Murakami *et al.*, Phys. Lett. B **463**, 333 (1999).
- [10] A. Alavi-Harati *et al.*, Phys. Rev. Lett. **87**, 021801 (2001).

- [11] T. Alexopoulos *et al.*, Phys. Rev. D **70**, 092006 (2004).
- [12] W.-M. Yao *et al.*, J. Phys. G **33**, 1 (2006).
- [13] A. Alavi-Harati *et al.*, Phys. Rev. D **67**, 012005 (2003).
- [14] A.J. Roodman, *Proceedings of the VII International Conference on Calorimetry* (World Scientific, Singapore, 1998).
- [15] C. Bown *et al.*, Nucl. Instrum. Methods Phys. Res., Sect. A **369**, 248 (1996).